Recent Gyrokinetic Simulations with GYRO: Bohm Transport in DIII-D, the Local Limit of Global Simulations, and Transport Across a Minimum-q Surface

J. Candy
General Atomics, San Diego, CA

JIFT Workshop and 21 COE Workshop
Kyodai-Kaikan, Kyoto, JAPAN
15-17 December 2003

in collaboration with: *R.E. Waltz, M.N. Rosenbluth, W. Dorland*

Outline

1. Brief description of GYRO.
2. **Comprehensive DIII-D Simulations**
3. **The Local Limit of Global Simulations**
4. **Transport is Smooth Across a Minimum-q Surface**

1. Brief description of GYRO

SciDAC Plasma Microturbulence Project (PMP)

Code	**Lab**	**Type**	**Flux-Tube**	**Global**	$\delta A_{\|\|}$	$\delta B_{\|\|}$	**Shape**
GS2	UM/IFS	Euler	x		x	x	x
GTC	PPPL	PIC		x			
TUBE	UCol	PIC	x		x		
PG3EQ	LLNL	PIC	x				
GYRO	GA	Euler	x	x	x		x

Description of GYRO: Algorithms

- GYRO solves the 5-dimensional **Gyrokinetic-Maxwell** equations in shaped (κ, δ, Δ) plasma geometry.
- Discretized on an **Eulerian** grid, and thus free of statistical noise.
- Radially **global**; able to accomodate arbitrary radial profile variation of $q(r)$, $T_i(r)$, $n_e(r)$, etc.
- Toroidally **spectral** (single-n to full torus) with field-aligned coordinates of Miller:

$$f(r,\varphi,\theta,\lambda,E) = \sum_n e^{-in[\varphi - q(r)\theta]} f_n(r,\theta,\lambda,E)$$

$$\text{such that} \quad (\mathbf{b}\cdot\nabla)[\varphi - q(r)\theta] = 0.$$

Description of GYRO: Algorithms

- **Electromagnetic** fluctuations with real electrons (m_i/m_e = 3600).
- Electron parallel motion treated **implicitly**, and other dynamics **explicitly**, using Implicit-Explicit (IMEX) Runge-Kutta time-integration scheme.
- Old explicit version documented in [1].

Description of GYRO: Performance Issues

- **GYRO is portable**. Build and runs on following machines with specification of single environment variable:
  - this laptop
  - GA Linux clusters (PII, PIII and P4).
  - NERSC, SDSC and ORNL IBM Power3
  - ORNL IBM Power4
  - ORNL SGI Itanium (Pat Worley, ORNL)
  - **ORNL Cray X1** (Mark Fahey, ORNL).
- 64 MSPs on Cray X1 better than 512 Power3 processors.
- Balanced performance on all architectures (IA32, PowerPC, Vector)

2. Comprehensive DIII-D Simulations

DIII-D Simulations: Reference Discharges

- For some time now, we have been studying Bohm-scaled **DIII-D L-mode discharges** 101381 ($\rho_* = 0.0025$) and 101391 ($\rho_* = 0.004$).
- Algorithmic refinements in combination with Implicit-Explicit Runge-Kutta scheme solved **electron box mode** problem and allowed operation at reasonable timestep (limited by nonlinear processes).
- Reruns of the DIII-D cases in early 2003 used real mass ratio ($m_i/m_e = 3600$) and all physics (finite-β, equilibrium sheared $\mathbf{E} \times \mathbf{B}$ rotation) operative [2].

DIII-D Simulations: Transport Stiffness

Sensitivity studies show so-called *transport stiffness* effect for changing dT_i/dr, even for electron transport:

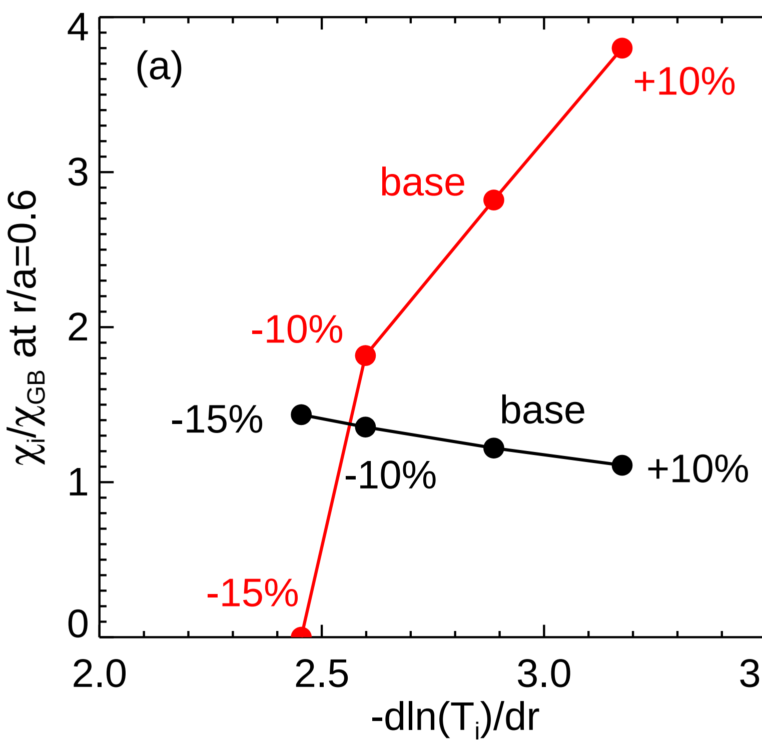

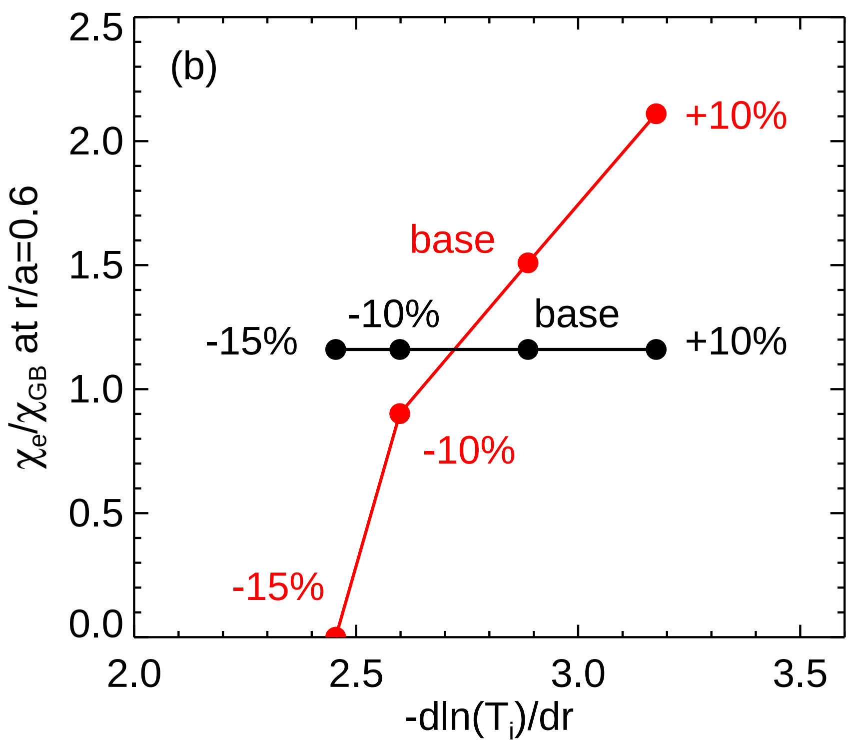

GENERAL ATOMICS

DIII-D Simulations: Best Results

Based on the sensitivity studies, we used -10% T_i' and re-ran at higher resolution to obtain a remarkable result for the full ion transport profile **[show movie]**:

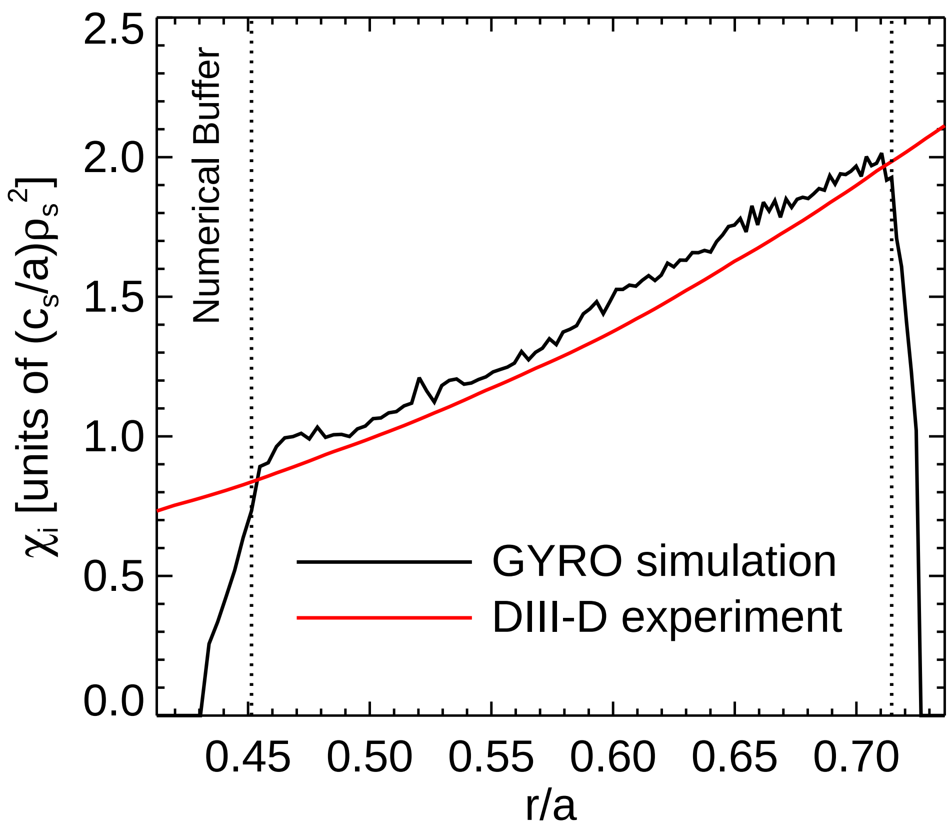

DIII-D Simulations: What is the effect of β?

For our DIII-D L-mode simulations, finite-β effects are strong in the core, but weak beyond $r/a = 0.6$ (and reduce electron layer response).

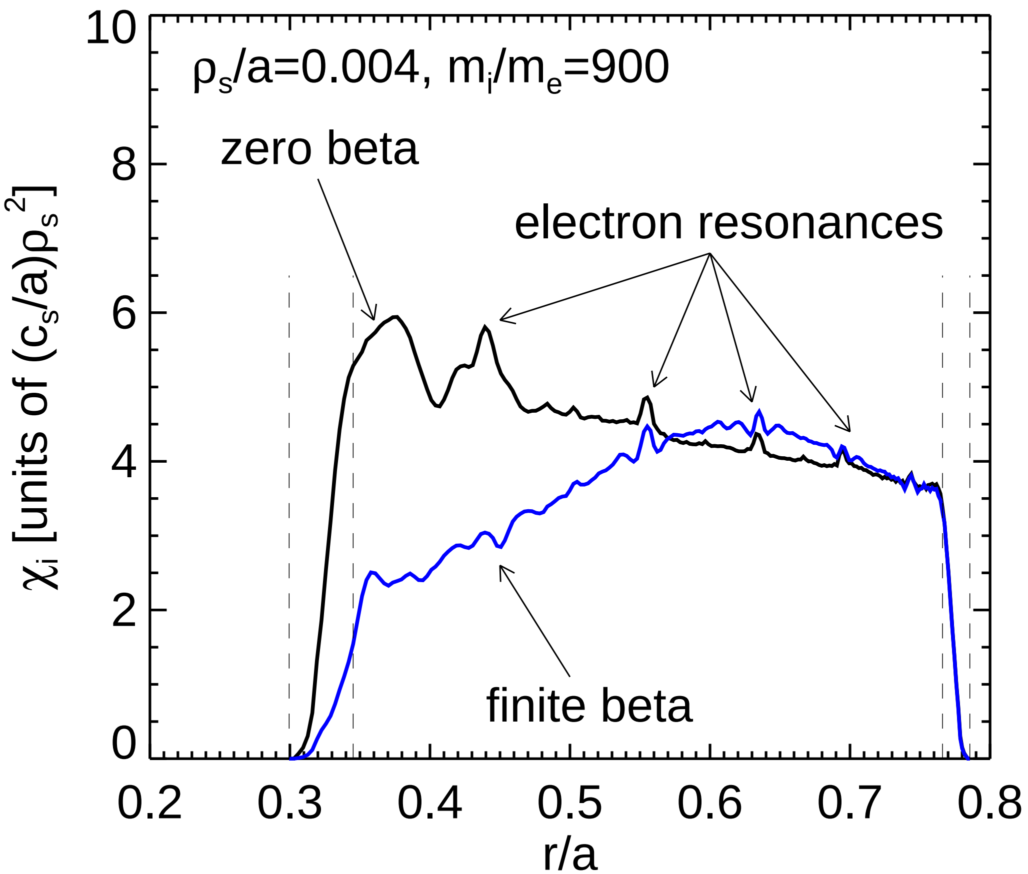

3. The Local Limit of Global Simulations

Local Limit: GTC runs presented in PRL

- Upon publication in PRL [3], it was apparent that GTC results at small ρ_* were not in agreement with **Cyclone local result** (PG3EQ, TUBE, GS2, GYRO).

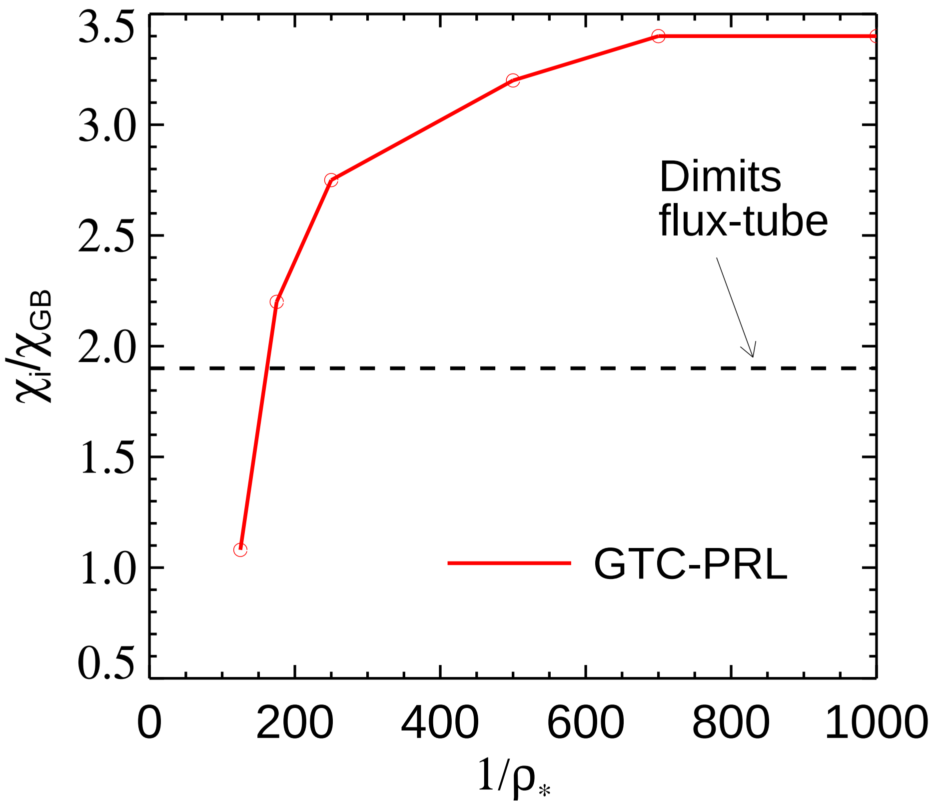

Local Limit: GTC runs presented at IAEA

- Subsequent IAEA results [4] showed the anomaly reduced but still apparent, leading to the question: **is there a problem with the local (flux-tube) limit?**

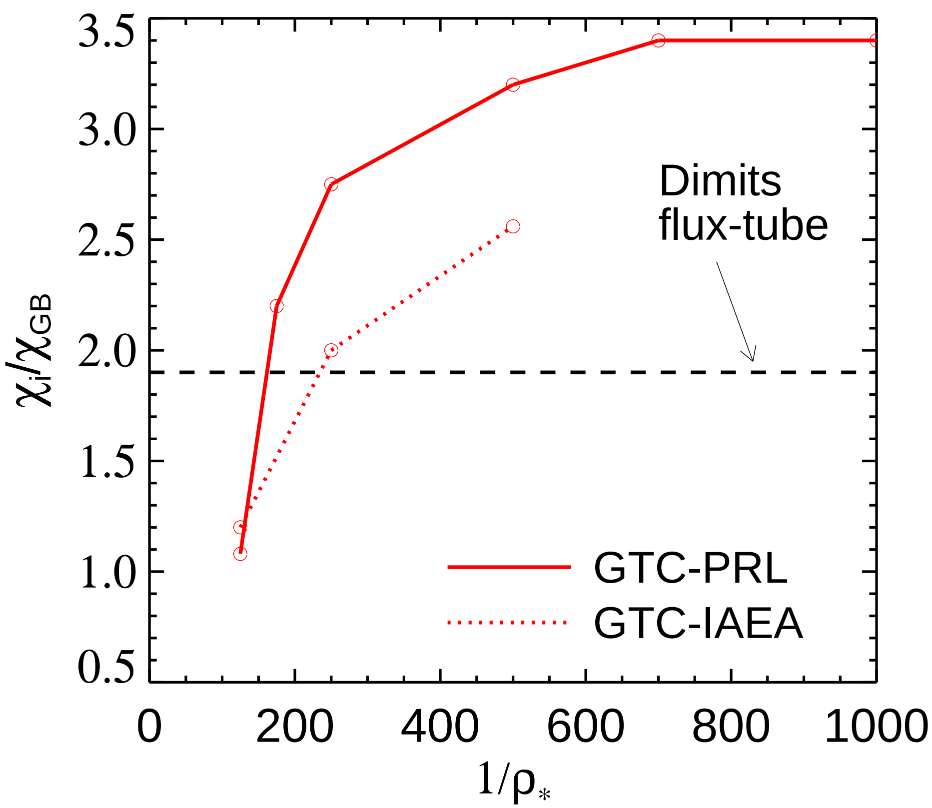

Possible Explanations

- The original GTC-PRL simulations used an unshifted circular geometry model which differed from the $s - \alpha$ model used by PG3EQ/TUBE/ GS2/GYRO in certain features.
- The IAEA work [4] (as we understand it) eliminated this difference, and then argued that the higher GTC value might be a consequence of nonperiodic boundary conditions, large radial domain size and radial variation of ω_*, q, s and r/R used in the latter calculation.
- Using the same radial profiles at the GTC case, we ran GYRO over a wide range of ρ_*. No matter what variations were tried, we recovered the local limit in all cases.

Local Limit Recovered

- All GYRO runs (and many, many were carried out over a one-year period) **confirmed the Cyclone value** as the upper bound.

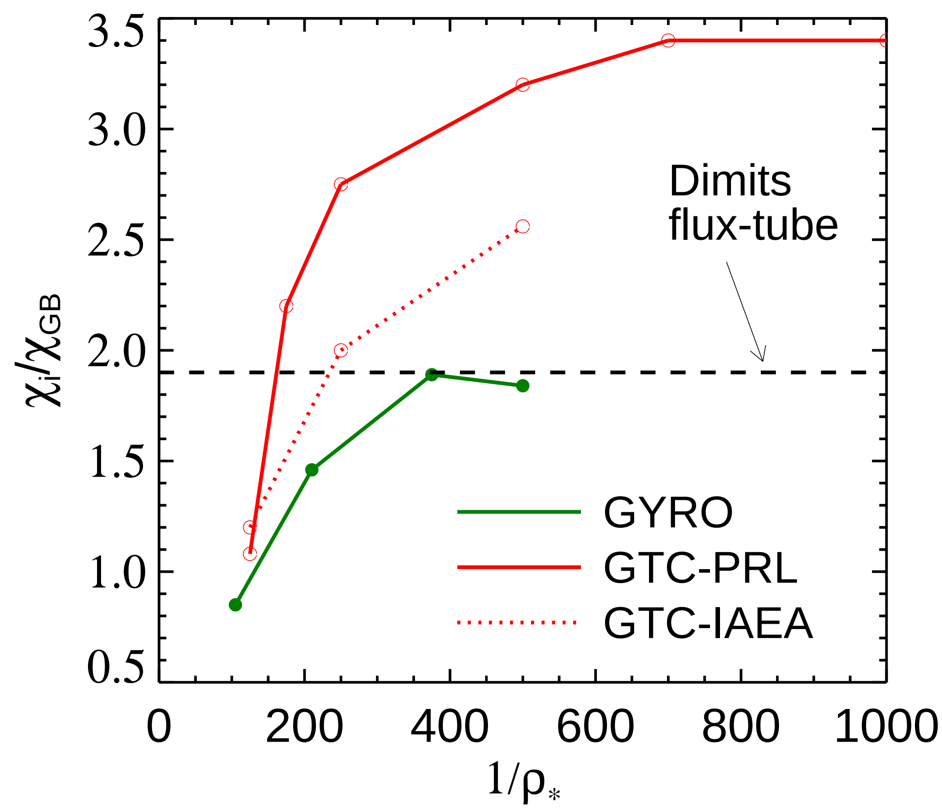

GENERAL ATOMICS

Comparison with GS2 Local Results

- **GS2 local runs** agree with global GYRO run at interior radii (left)
- **Beware:** Long-time averages are required to achieve statistical steady-state at large system-size (right)

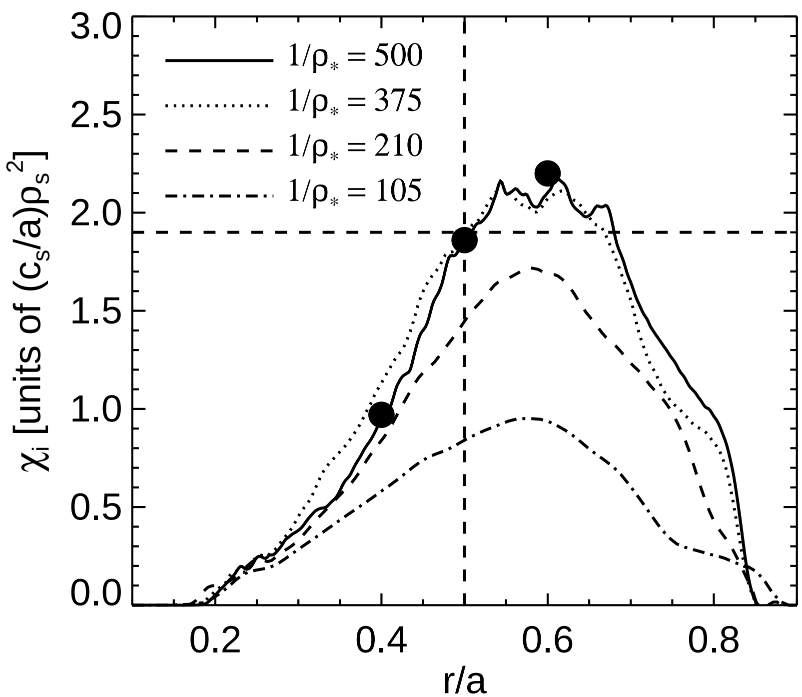

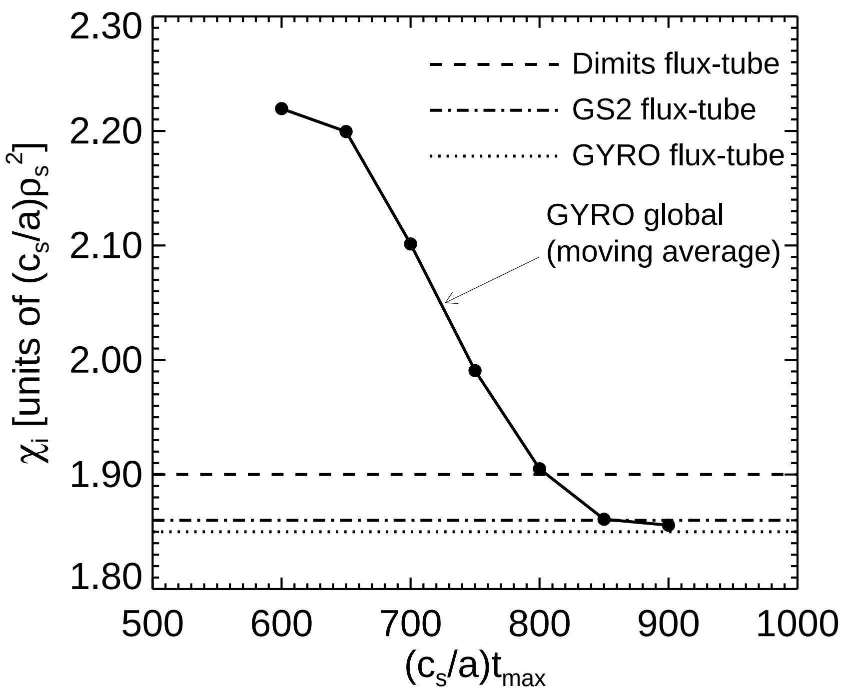

GENERAL ATOMICS

A Word About Radial Profiles

- The customary setup [5, 6, 7, 3, 8, 9] for global simulations puts the largest instability drive at the centre of the simulation domain, with vanishing drive in the vicinity of the simulation boundary.
- **In experiments, however, $1/L_T$ does not show this trend but rather tends to increase from core to edge, rising sharply near the edge.**

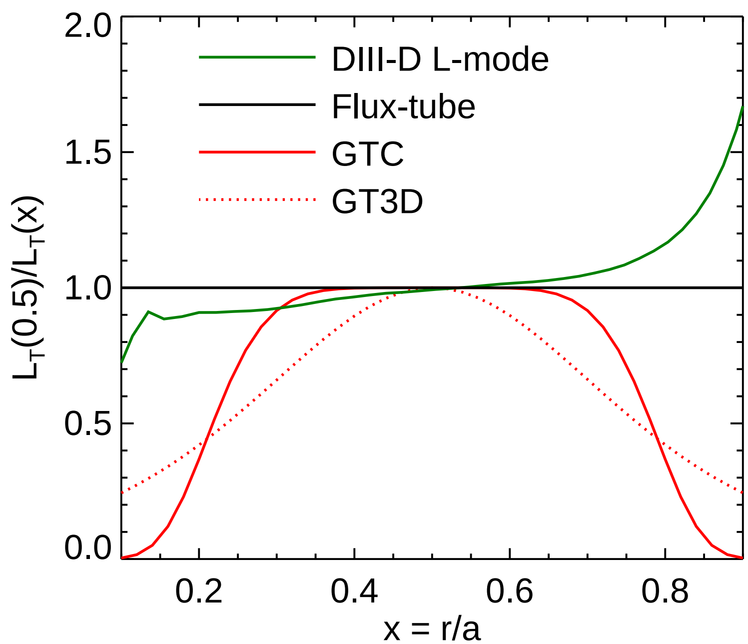

GENERAL ATOMICS

Artificial Profile Shear Can Alter Scaling

- The use of a ramped temperature gradient profile gives rise to a transition at larger ρ_*:

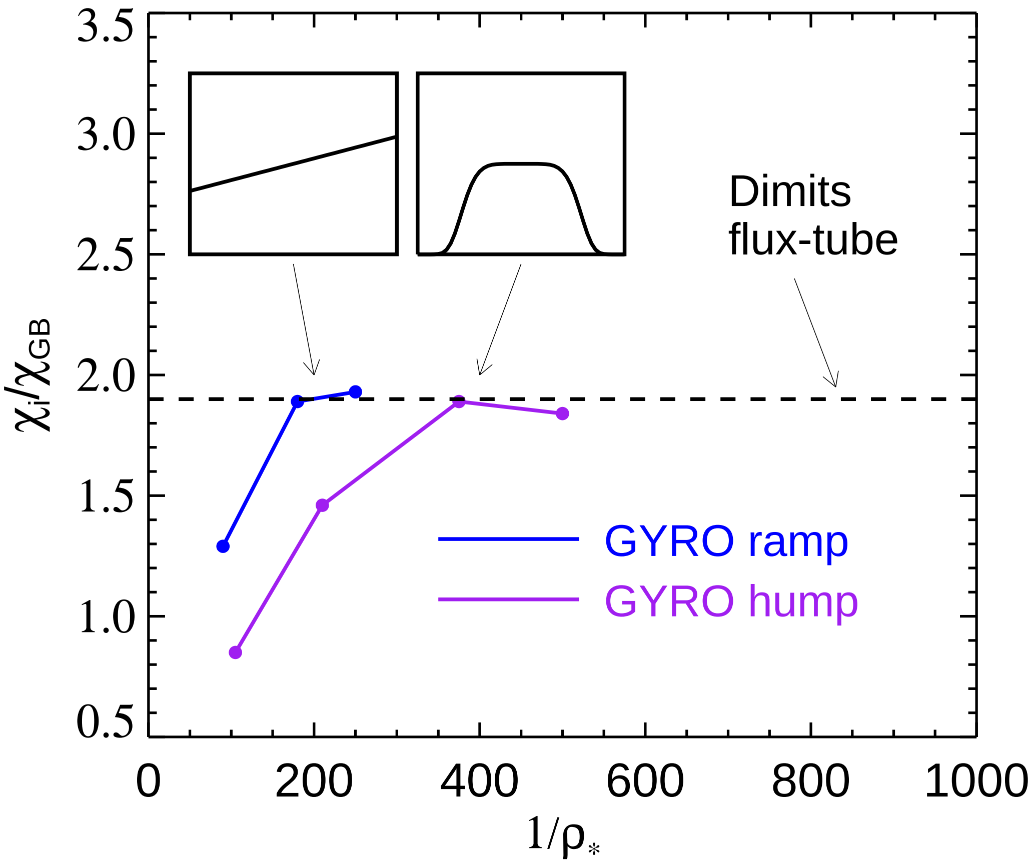

3. Transport is Smooth Across a Minimum-q Surface.

Local Modes in Extended Angle

- Local simulations by Waltz (circa 1995) [15] showed that as magnetic shear, s, in increased from negative to positive values, $\chi_i(s)$ increases monotonically through zero.
- We wanted to understand if this trend peristed at finite ρ_* in a global simulation which contains a minimum-q $(s = 0)$ region.
- **The results which we show consider only adiabatic electrons and simple ITG physics with no equilibrium sheared $\mathrm{E} \times \mathrm{B}$ rotation.**

Local Modes in Extended Angle

- Ballooning eigenmodes, ϕ_B, for $s = 1.0$ (left) and $s = 0.05$ (right).
- **Ballooning eigenmodes becomes periodic in θ_p as $s \to 0$.**

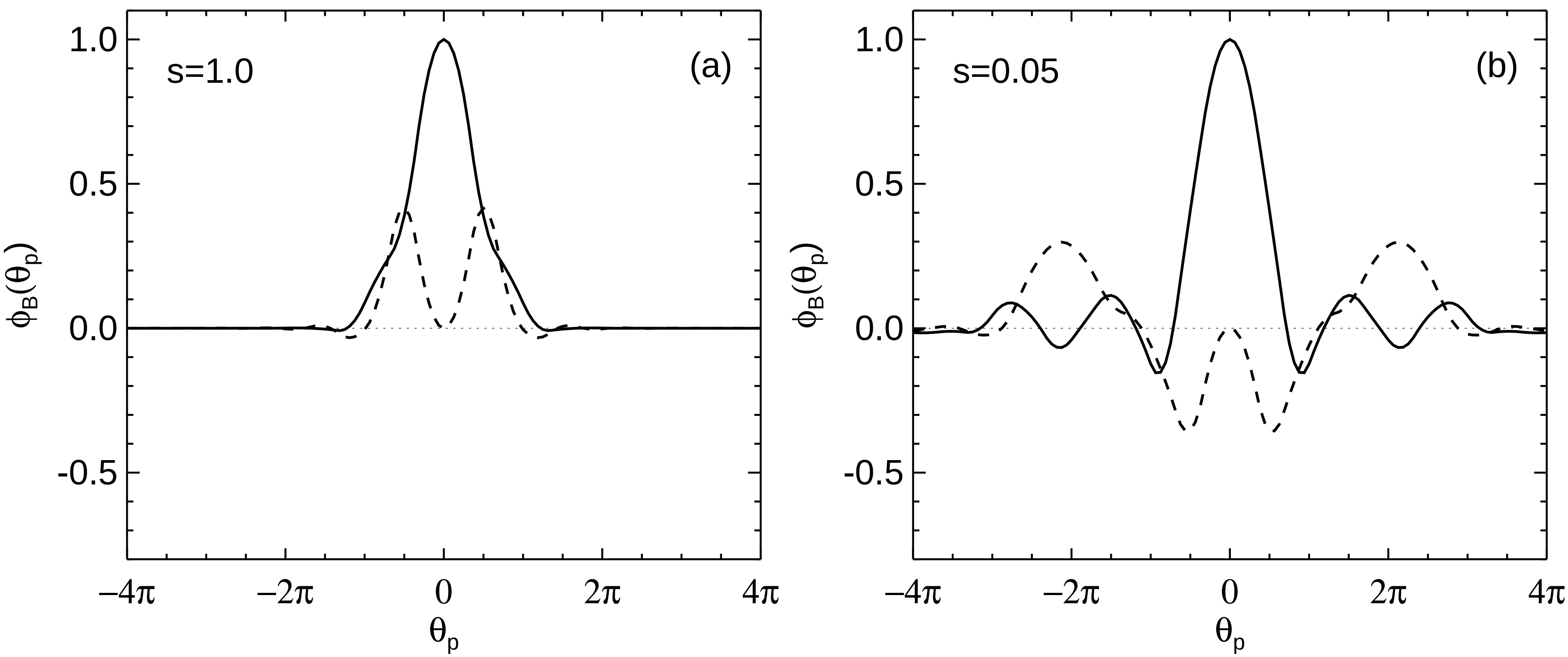

GENERAL ATOMICS

Poloidal Harmonics of Local Modes

Poloidal harmonics for $s = 1.0$ (left) and $s = 0.05$ (right).

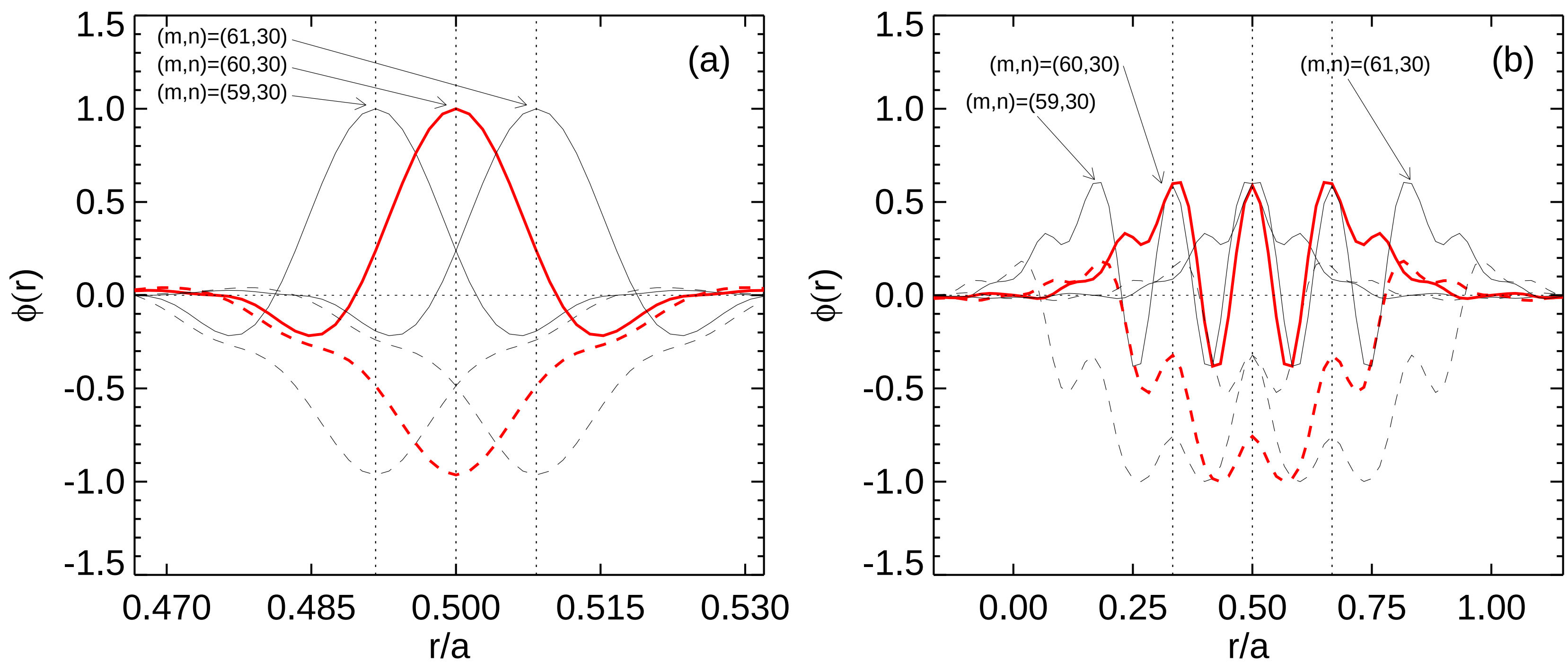

Local theory gives extended, complicated modes (actually, Mathieu functions) at low shear.

Weak-shear Eigenvalue

- When ω is larger than the ion drift and transit and transit frequencies, the ITG ballooning equation [10, 11] can be solved to yield

$$\hat{\boldsymbol{\omega}} = \hat{\boldsymbol{\omega}}_{\mathbf{0}} + \boldsymbol{\lambda}_{\mathbf{1}} \boldsymbol{s} + \boldsymbol{\lambda}_{\mathbf{2}} |\boldsymbol{s}| \tag{1}$$

- Above, $\hat{\omega}_0 = \hat{\omega}_{00} - F(\hat{\omega}_{00})$ and $\lambda_1 = F(\hat{\omega}_0)$, with

$$\hat{\omega}_{00} = \omega_R + i\sqrt{\frac{2\epsilon_n(1+\eta_i)}{1+\hat{k}^2} - \omega_R^2} \quad , \quad \omega_R = \frac{1-2\epsilon_n - \hat{k}^2(1+\eta_i)}{2(1+\hat{k}^2)} \tag{2}$$

$$\text{and} \quad F(z) = \frac{\sqrt{\epsilon_n z}}{2q\hat{k}} \left[1 - \frac{z^2}{2\,\epsilon_n} \frac{\eta_i + 2}{(z+\eta_i+1)^2} \right]^{-1} \tag{3}$$

Analytical and Numerical Eigenmodes

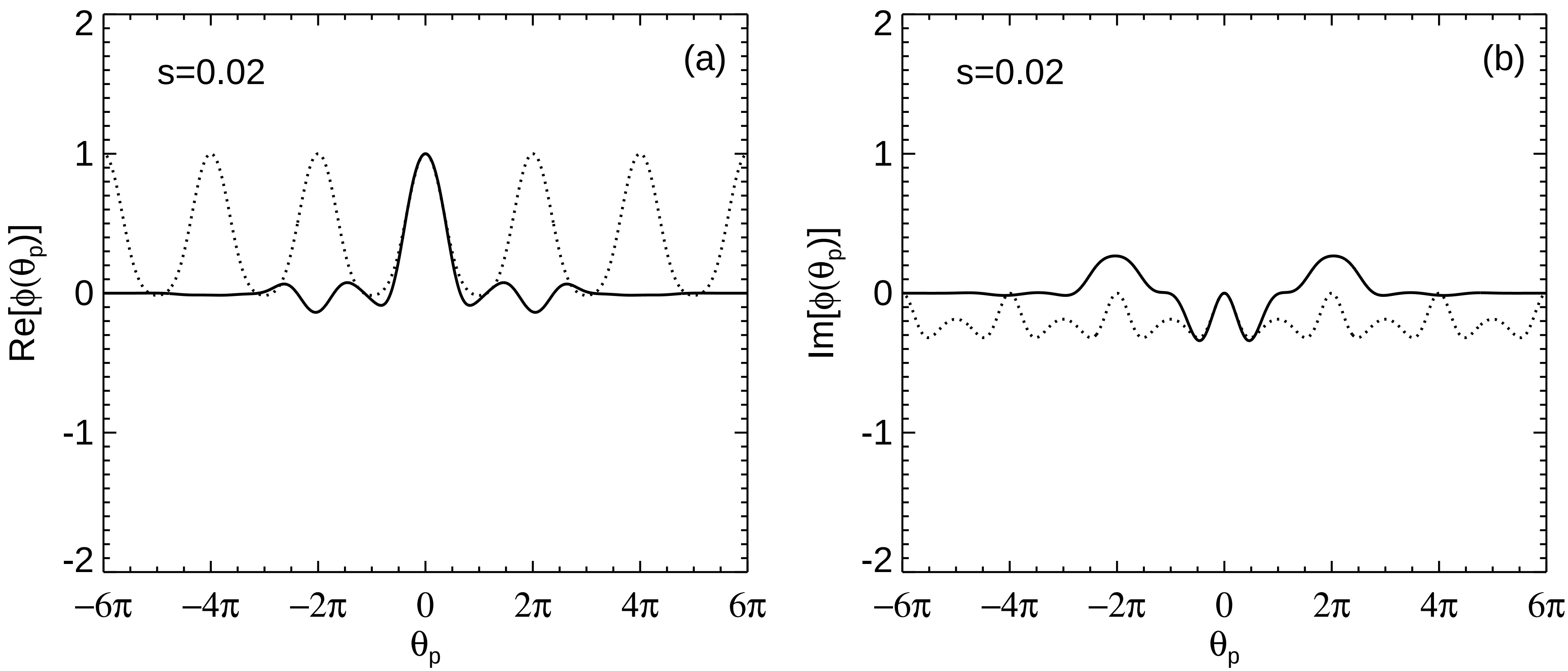

Analytical and Numerical Eigenmodes

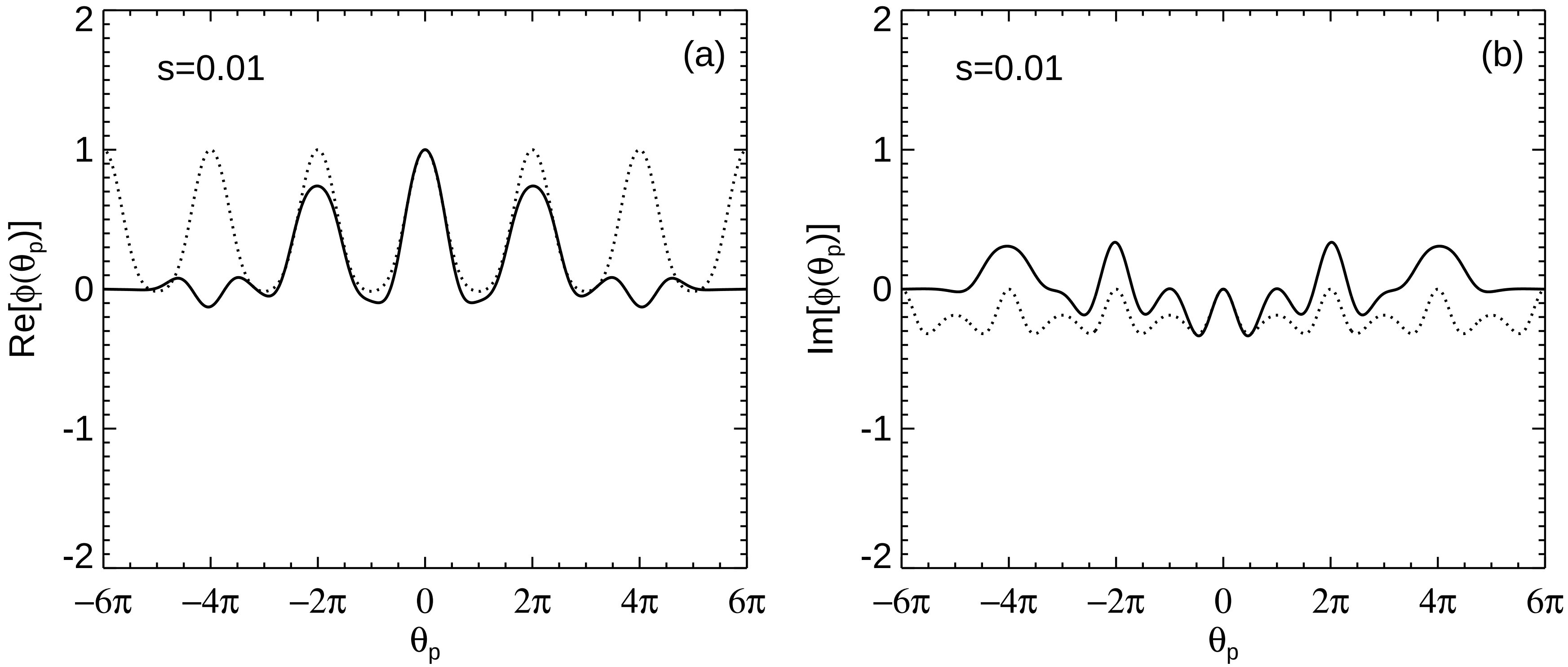

Zero-Shear Gap Theory of ITB Formation

- In the literature, we found what we tentatively call the Zero-Shear Gap (ZSG) theory of ITB formation [12, 13].
- In the context of ZSG, an absence of toroidal coupling in the gap region is posited to preclude the development of a “global structure of the toroidal mode” [14]:
- We found this to be a novel idea, and wished to reconcile this idea with earlier local simulations by Waltz which showed that transport smoothly increases across the point $s = 0$ [15].

Rational Surface Gap

- ZSG theory focuses on an ostensible rarefaction of resonant surfaces (for a given n) in the neighborhood of $s = 0$:

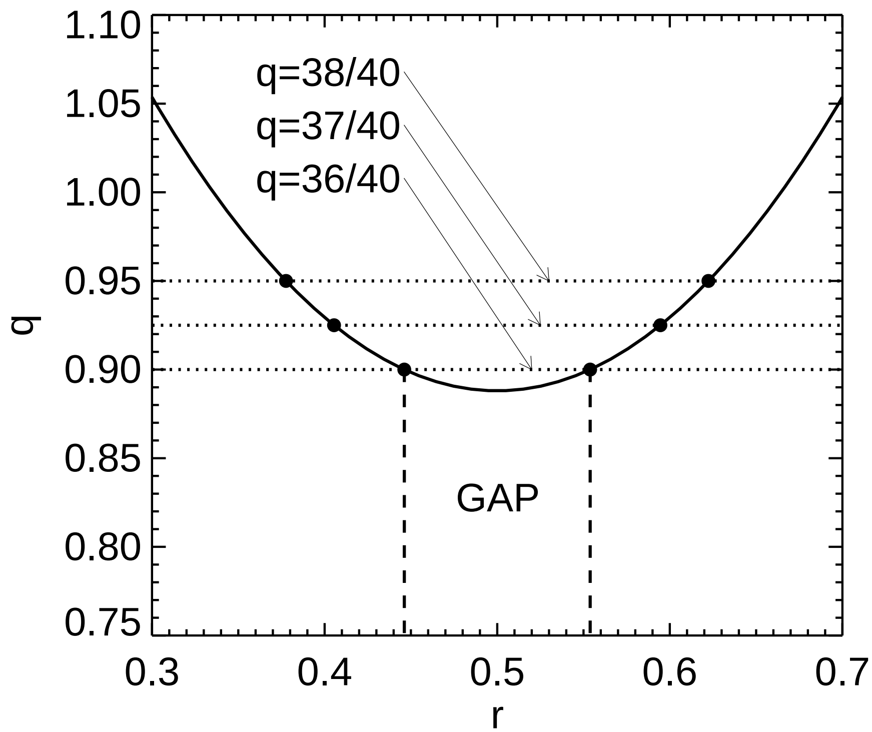

Is There Evidence for ZSG Theory?

- Various works espousing ZSG theory [16, 14, 12] are supplemented by toroidal PIC simulations.
- It is difficult to draw solid conclusions from any of those simulations since no curves of $\chi_i(r)$ are given (only electrostatic potential profiles are shown).
- The use of a strongly peaked temperature profile in [16, 14], with the peaking inside the $s = 0$ surface, makes it impossible for the reader to differentiate gap effects from pressure gradient effects.
- The added claim that the presence of sheared equilibrium poloidal flow can make the barrier more "efficient" is *non sequitur*. A strong effect of flow shear on the barrier dynamics implies that the flow shear is a cause of transport barrier formation in and of itself.

Local Modes to the Left and Right

Case	r/a	s	q	n	$k_\theta \rho_s$	$(a/c_s)\gamma$
Negative shear	0.4	-0.356	0.929	32	0.297	0.05
Positive shear	0.6	+0.356	0.929	48	0.297	0.11

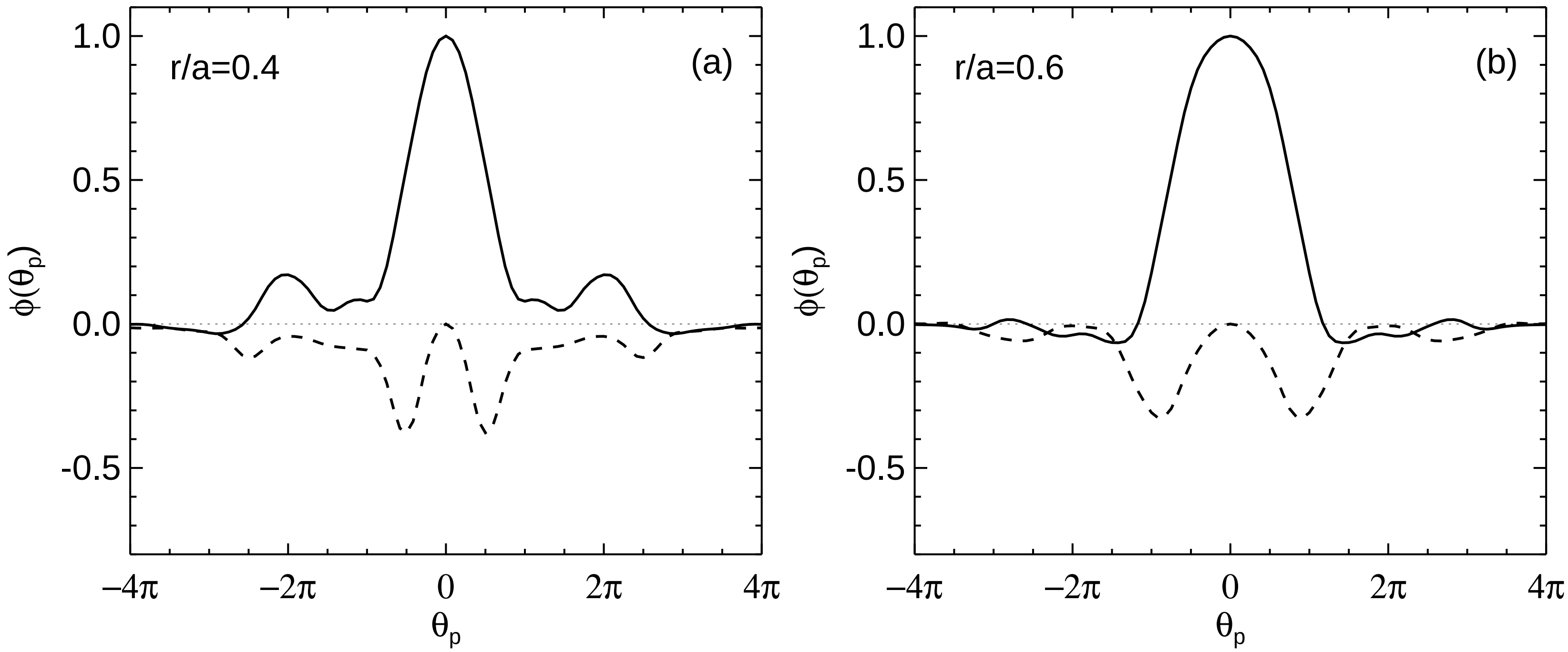

GENERAL ATOMICS

Poloidal harmonics: Linear and Nonlinear

- Neither linear (top) nor nonlinear (bottom) runs show a gap.

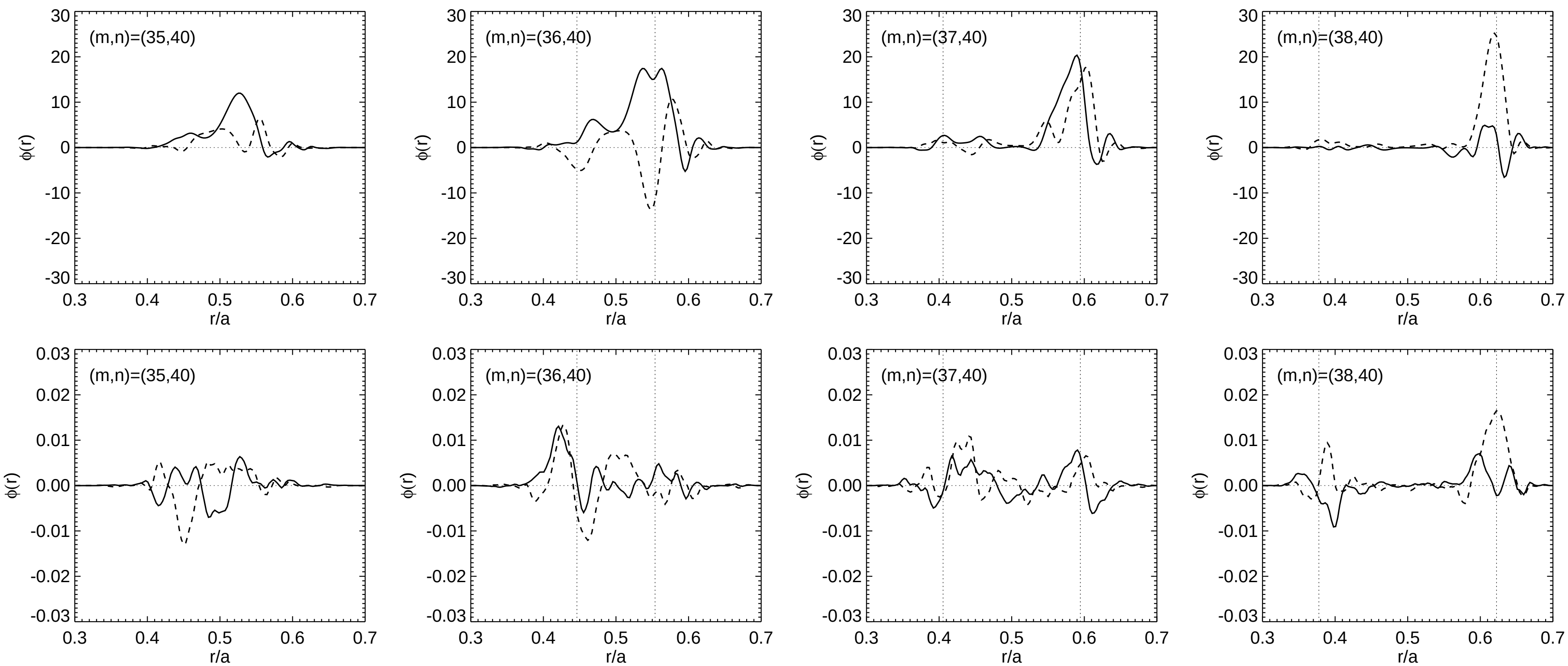

GENERAL ATOMICS

Calculation of $\chi_i(r)$

- The indicator for the onset of an ITB in this context ought to be a drop in $\chi_i(r)$ in the gap region.
- **We see no such drop in any simulations.**
- **In reality, local (flux-tube) nonlinear simulations are a good approximation to the global results, even in the vicinity of $s = 0$.**
- The approximation improves as ρ_* decreases.

Comparison of Local and Global Simulations

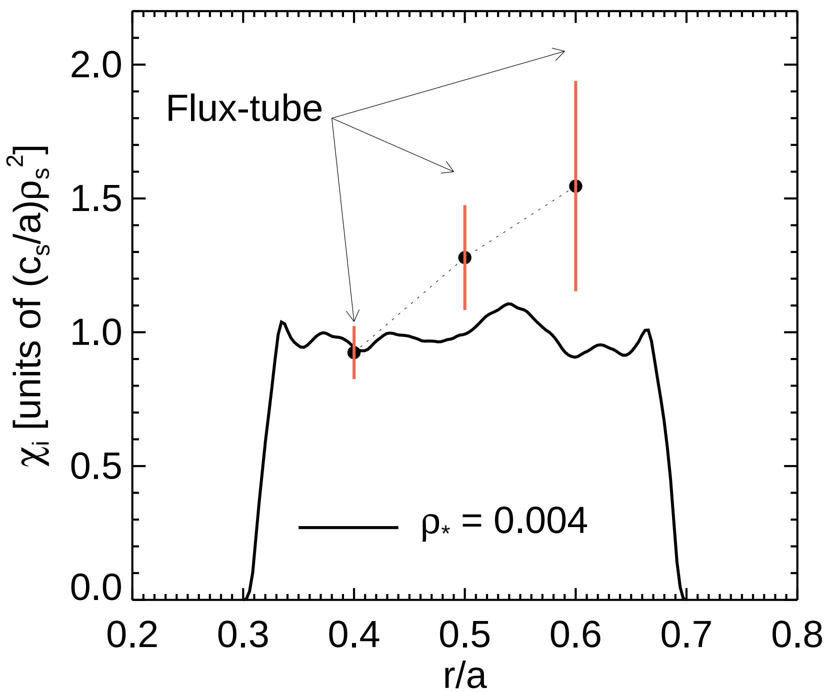

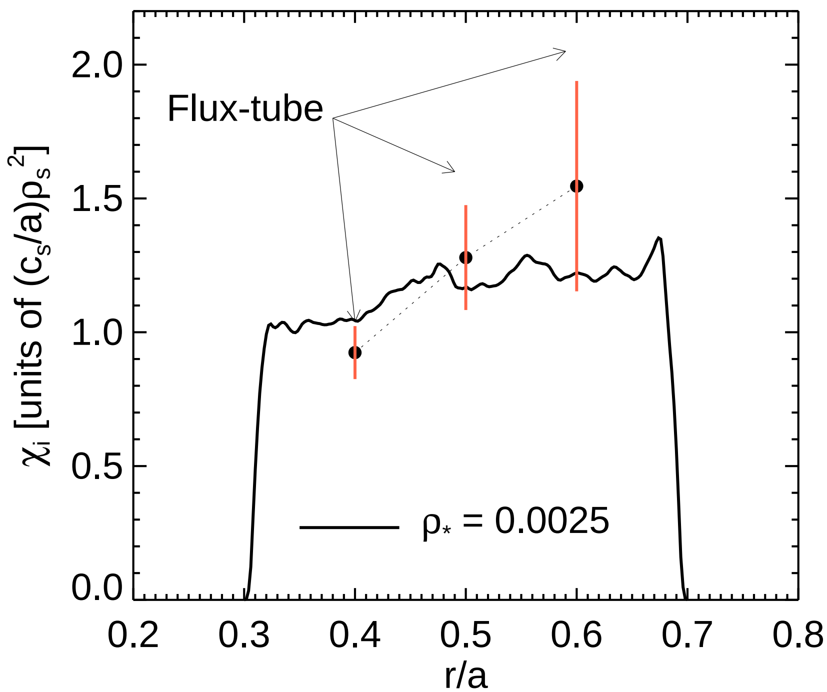

Confluence of local and Global Results

Flux-tube runs were done at low resolution – increased toroidal resolution will raise numbers slightly.

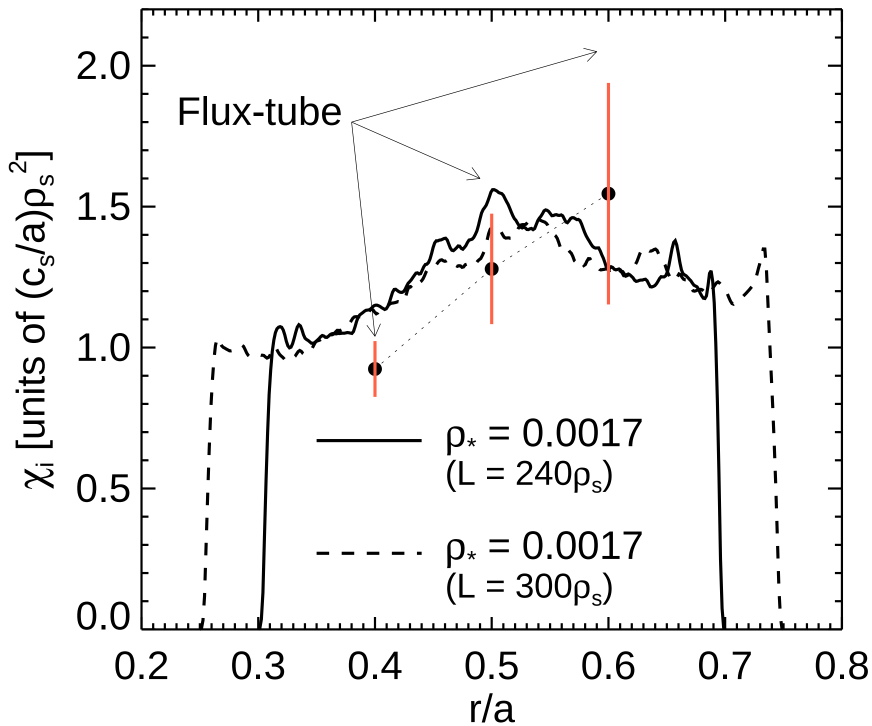

Results are insensitive to box size at $\rho_* = 0.0017$.

References

[1] J. Candy and R.E. Waltz. *J. Comput. Phys.* **186**, 545 (2003).

[2] J. Candy and R.E. Waltz. *Phys. Rev. Lett.* **91**, 045001–1 (2003).

[3] Z. Lin, S. Ethier, T.S. Hahm, and W.M. Tang. *Phys. Rev. Lett.* **88**, 195004 (2002).

[4] Z. Lin, T.S. Hahm, S. Ethier, W.W. Lee, J. Lewandowski, G. Rewoldt, W.M. Tang, W.X. Wang, L. Chen, and P.H. Diamond. in *Plasma Physics and Controlled Nuclear Fusion Research (Proc. 19th International Conference on Fusion Energy, Lyon, 2002)*. IAEA, Vienna, (2003).

[5] S. Brunner, M. Fivaz, T.M. Tran, and J. Vaclavic. *Phys. Plasmas* **5**, 3929 (1998).

[6] Z. Lin, T.S. Hahm, W.W. Lee, W.M. Tang, and R.B. White. *Science* **281**, 1835 (1998).

[7] Z. Lin, T.S. Hahm, W.W. Lee, W.M. Tang, and P.H. Diamond. *Phys. Rev. Lett.* **83**, 3645 (1999).

[8] Y. Idomura, S. Tokuda, and Y. Kishimoto. *New. J. Phys.* **4**, 101.1 (2002).

[9] Y. Idomura, S. Tokuda, and Y. Kishimoto. *Nucl. Fusion* **43**, 234 (2003).

[10] R.J. Hastie, K.W. Hesketh, and J.B. Taylor. *Nucl. Fusion* **19**, 1223 (1979).

[11] C.Z. Cheng and K.T. Tsang. *Nucl. Fusion* **21**, 643 (1981).

[12] Y. Kishimoto, J.-Y. Kim, W. Horton, T. Tajima, M.J. LeBrun, S.A. Dettrick, J.Q. Li, and S. Shirai. *Nucl. Fusion* **40**, 667 (2000).

[13] X. Garbet, C. Bourdelle, G.T. Hoang, P. Maget, S. Benkadda, P. Beyer, C. Figarella, I. Voitsekovitch, O. Agullo, and N. Bian. *Phys. Plasmas* **8**, 2793 (2001).

[14] Y. Kishimoto, J.-Y. Kim, W. Horton, T. Tajima, M.J. LeBrun, and S. Shirai. *Plasma Phys. Controlled Fusion* **40**, A663 (1998).

[15] R.E. Waltz, G.R. Kerbel, J. Milovich, and G.W. Hammett. *Phys. Plasmas* **2**, 2408 (1995).

[16] Y. Kishimoto, J.-Y. Kim, T. Fukuda, S. Ishida, T. Fujita, T. Tajima, W. Horton, G. Furnish, and M.J. LeBrun. in *Plasma Physics and Controlled Nuclear Fusion Research (Proc. 16th International Conference on Fusion Energy, Montréal, 1996)*, 581. IAEA, Vienna, 1997.